2D Assembly of Metallacycles on HOPG by Shape-Persistent Macrocycle Templates

Ting Chen,[†] Ge-Bo Pan,*[‡] Henning Wettach,[§] Martin Fritzsche,[§] Sigurd Höger,*[§] Li-Jun Wan,*[†] Hai-Bo Yang,[∥] Brian H. Northrop,[∥] and Peter J. Stang[∥]

Suzhou Institute of Nano-tech and Nano-bionics, Chinese Academy of Sciences, Suzhou 215125, P. R. China, Kekulé-Institut für Organische Chemie und Biochemie, Rheinische Friedrich-Wilhelms-Universität Bonn, Gerhard-Domagk-Strasse 1, 53121 Bonn, Germany, Institute of Chemistry, Chinese Academy of Sciences, Beijing 100190, P. R. China, and Department of Chemistry, University of Utah, 315 South 1400 East, Salt Lake City, Utah 84112

Received August 26, 2009; E-mail: gbpan2008@sinano.ac.cn; hoeger@uni-bonn.de; wanlijun@iccas.ac.cn

Abstract: The synthesis and scanning tunneling microscopy (STM) investigations of shape-persistent arylene-ethynylene-butadiynylene macrocycles along with their codeposites with metallacycles are reported. 2D ordered arrays of macrocycles and macrocycle/metallacycle architectures (1:1) have been obtained on HOPG by self-assembly under ambient conditions. It is found that the ordered macrocycle array acts as a template for the deposition of the adlayer molecules. For each underlying macrocycle, one metallacycle has been detected. The unit-cell data of both, the macrocycles and their codeposites, show that the structural information of the macrocycle layer is perfectly transformed to the guest molecules. A rather unexpected observation is that the present compound could not be coadsorbed with C_{60}, indicating that only a minor change in the structure of the macrocycle has a dramatic effect on the ability of the monolayer to bind additional guest molecules.

Introduction

Self-assembly as an important way to create ordered nanoscale structures and molecule-based devices has attracted considerable attention in materials science.[1] However, this approach toward complex molecular structures on solid surfaces is still a great challenge and requires not only the assembly of a single molecule but the (predictable) formation of multicomponent assemblies. Therefore, the investigation of codeposits of two or more molecular compounds on solid surfaces is currently a highly attractive field of research, mostly performed by scanning tunneling microscopy (STM).[2,3] Shape-persistent macrocycles are promising building blocks in that context. Their backbone can be electron-deficient or electron-rich, and their interior as well as their exterior can be functionalized independently.[4] This allows for utilizing the macrocycle pattern as a template for the assembly of guest molecules with complementary size, electron affinity, or functionalization.[5] Although the coadsorption of rigid macrocycles with fullerenes and flat organic molecules has recently been described by us and other groups, the formation of adlayers of metallacycles onto rigid macrocycle templates has not been described so far.[6,7] In this work, we report the synthesis and STM investigations of shape-persistent arylene-ethynylene-butadiynylene macrocycles **1** and **2** along with their codeposites with the metallacycles **3** and **4**.[8]

Results and Discussion

Synthesis. Scheme 1 displays the synthesis of the shape-persistent macrocycles **1** and **2** (experimental details are given

[†] Institute of Chemistry, Chinese Academy of Sciences.
[‡] Suzhou Institute of Nano-tech and Nano-bionics, Chinese Academy of Sciences.
[§] Rheinische Friedrich-Wilhelms-Universität Bonn.
[∥] University of Utah.

(1) (a) Service, R. F. *Science* **2005**, *309*, 95. (b) Lehn, J. M. *Supramolecular Chemistry*; VCH: Weinheim, Germany, 1995. (c) Alivisatos, A. P.; Barbara, P. F.; Castleman, A. W.; Chang, J.; Dixon, D. A.; Klein, M. L.; McLendon, G. L.; Miller, J. S.; Ratner, M. A.; Rossky, P. J.; Stupp, S. I.; Thompson, M. E. *Adv. Mater.* **1998**, *10*, 1297. (d) Ariga, K.; Hill, J. P.; Lee, M. V.; Vinu, A.; Charvet, R.; Acharya, S. *Sci. Technol. Adv. Mater.* **2008**, *9*, 014109.
(2) (a) De Feyter, S.; De Schryver, F. C. *Chem. Soc. Rev.* **2003**, *32*, 139. (b) Wan, L. J. *Acc. Chem. Res.* **2006**, *39*, 334. (c) Müllen, K.; Rabe, J. P. *Acc. Chem. Res.* **2008**, *41*, 511. (d) Barth, J. V.; Constantine, G.; Kern, K. *Nature* **2005**, *437*, 671. (e) Surin, M.; Samori, P.; Jouaiti, A.; Kyritsakas, N.; Hosseini, M. W. *Angew. Chem.* **2006**, *119*, 249. (f) Hermann, B. A.; Scherer, L. J.; Housecroft, C. E.; Constable, E. C. *Adv. Funct. Mater.* **2006**, *16*, 221.
(3) (a) Pan, G.-B.; Liu, J.-M.; Zhang, H.-M.; Wan, L.-J.; Zheng, Q.-Y.; Bai, C.-L. *Angew. Chem.* **2003**, *115*, 2853. (b) Surin, M.; Samori, P. *Small* **2007**, *3*, 190. (c) Adisoejoso, J.; Tahara, K.; Okuhata, S.; Lei, S.; Tobe, Y.; De Feyter, S. *Angew. Chem.* **2009**, *121*, 7489. (d) Michl, J.; Magnera, T. F. *Proc. Natl. Acad. Sci. U.S.A.* **2002**, *99*, 4788. (e) De Feyter, S.; Abdel-Mottaleb, M. M. S.; Schuurmans, N.; Verkuijl, B. J. V.; van Esch, J. H.; Feringa, B. L.; De Schryver, F. C. *Chem.—Eur. J.* **2004**, *10*, 1124. (f) Piot, L.; Marchenko, A.; Wu, J.; Müllen, K.; Fichou, D. *J. Am. Chem. Soc.* **2005**, *127*, 16245. (g) Kikkawa, Y.; Koyama, E.; Tsuzuki, S.; Fujiwara, K.; Miyake, K.; Tokuhisa, H.; Kanesato, M. *Langmuir* **2006**, *22*, 6910. (h) Yang, Y.-L.; Wang, C. *Int. J. Nanotechnol.* **2007**, *4*, 4. (hh) Furukawa, S.; De Feyter, S. *Top. Curr. Chem.* **2009**, *287*, 87. (i) MacLeod, J. M.; Ivasenko, O.; Fu, C.; Taerum, T.; Rosei, F.; Perepichka, D. F. *J. Am. Chem. Soc.* **2009**, *131*, 16844.
(4) (a) Höger, S. *J. Polym. Sci., Part A: Polym. Chem.* **1999**, *37*, 2685. (b) Haley, M. M.; Pak, J. J.; Brand, S. C. *Top. Curr. Chem.* **1999**, *201*, 81. (c) Grave, C.; Schlüter, A. D. *Eur. J. Org. Chem.* **2002**, 3075. (d) Zhao, D.; Moore, J. S. *Chem. Commun.* **2003**, 807. (e) Moore, J. S. *Acc. Chem. Res.* **1997**, *30*, 402. (f) Höger, S. *Chem.—Eur. J.* **2004**, *10*, 1320. (g) *Acetylene Chemistry*; Diederich, F., Stang, P. J., Tykwinsky, R. R., Eds.; Wiley-VCH: Weinheim, Germany, 2005. (h) Zhang, W.; Moore, J. S. *Angew. Chem.* **2006**, *118*, 4524.

Scheme 1. Synthesis of **1** and **2**[a]
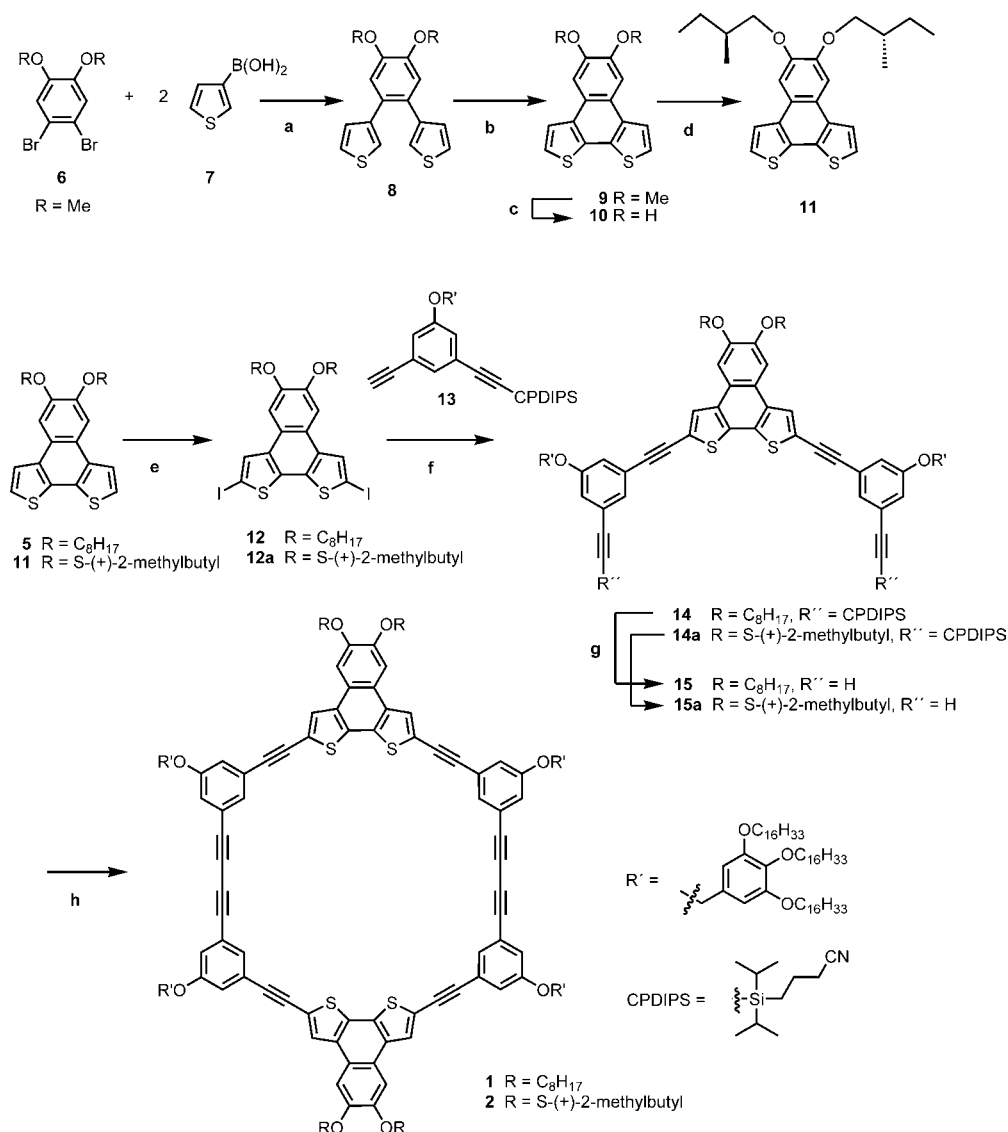
[a] (a) [Pd(PPh$_3$)$_4$], Na$_2$CO$_3$, toluene, EtOH, H$_2$O, reflux, 8 h; then 70 °C, 16 h, 83%; (b) 1.) FeCl$_3$, CH$_2$Cl$_2$, CH$_3$NO$_2$, rt, 40 min, 2.) MeOH, rt, 1 h, 19%; (c) BBr$_3$, CH$_2$Cl$_2$, −78 °C to rt, 100%; (d) (S)-(+)-1-bromo-2-methylbutane, K$_2$CO$_3$, KI, DMF, 65 °C, 2 d, 60%; (e) *n*-BuLi, TMEDA, I$_2$, THF, −78 °C to rt, **12**: 90%, **12a**: 87%; (f) [PdCl$_2$(PPh$_3$)$_2$], CuI, PPh$_3$, THF, piperidine, rt, 2 d, **14**: 93%, **14a**: 97%; (g) TBAF, THF, rt, 2 h, **15**: 91%,**15a**: 80%; (h) CuCl, CuCl$_2$, pyridine, 40 °C, 96 h, **1**: 20%, **2**: 3%.

in the Supporting Information), which are based on the phenylene−ethynylene−butadiynylene backbone. Bithiophene **5** was previously described in the literature and prepared accordingly.[9] For the synthesis of the bithiophene **11** an alternative approach was worked out in which the (chiral) side groups were attached to the condensed heterocyclic core at the last step of the reaction sequence. Suzuki-coupling of 1,2-dibromo-4,5-dimethoxy benzene (**6**) with commercial available 3-thiophene boronic acid (**7**) and subsequent Fe(III) mediated thiophene−thiophene coupling lead to the dimethoxy compound **9** that was demethylated with boron tribromide to give the diol **10**. Alkylation with the corresponding alkyl bromide gave **11**. This reaction sequence allows a side group variation at a later stage of the synthesis and guarantees a high synthetic flexibility. Pd-catalyzed Sonogashira-Hagihara coupling of **5** (**11**) with the monoprotected bisacetylene **13** and subsequent fluoride induced deprotection of the silyl groups generated the bisacetylenic "half rings" **15a** and **15b**, respectively. For the macrocycle synthesis, the corresponding "half rings" were oxidatively dimerized under

pseudo high-dilution conditions by adding a dilute solution of the corresponding bisacetylene in pyridine over four days to a slurry of CuCl/CuCl$_2$ in the same solvent.[10] Purification of the macrocylces was achieved by column chromatography on silica gel and subsequent recycling GPC (see the Supporting Information).

STM Investigations. Figure 1 shows the molecular structures of **1**−**4** and their corresponding space-filling models with calculated molecular sizes. **1** and **2** contain (electron-rich) polycyclic bithiophene units in the backbone. Highly ordered arrays of the macrocycles on HOPG have been fabricated by self-assembly and characterized by STM. In brief, for the macrocycle arrays, a drop of a macrocycle solution in 1-phenyloctane was deposited onto the freshly cleaved surface of HOPG and then directly used for STM measurements.

Figure 2a represents a typical STM image of long-range-ordered monolayers of **1**. Different domains usually cross each other at an angle of 60 or 120°. The bright protrusions in the STM image are attributed to the unsaturated backbone of the
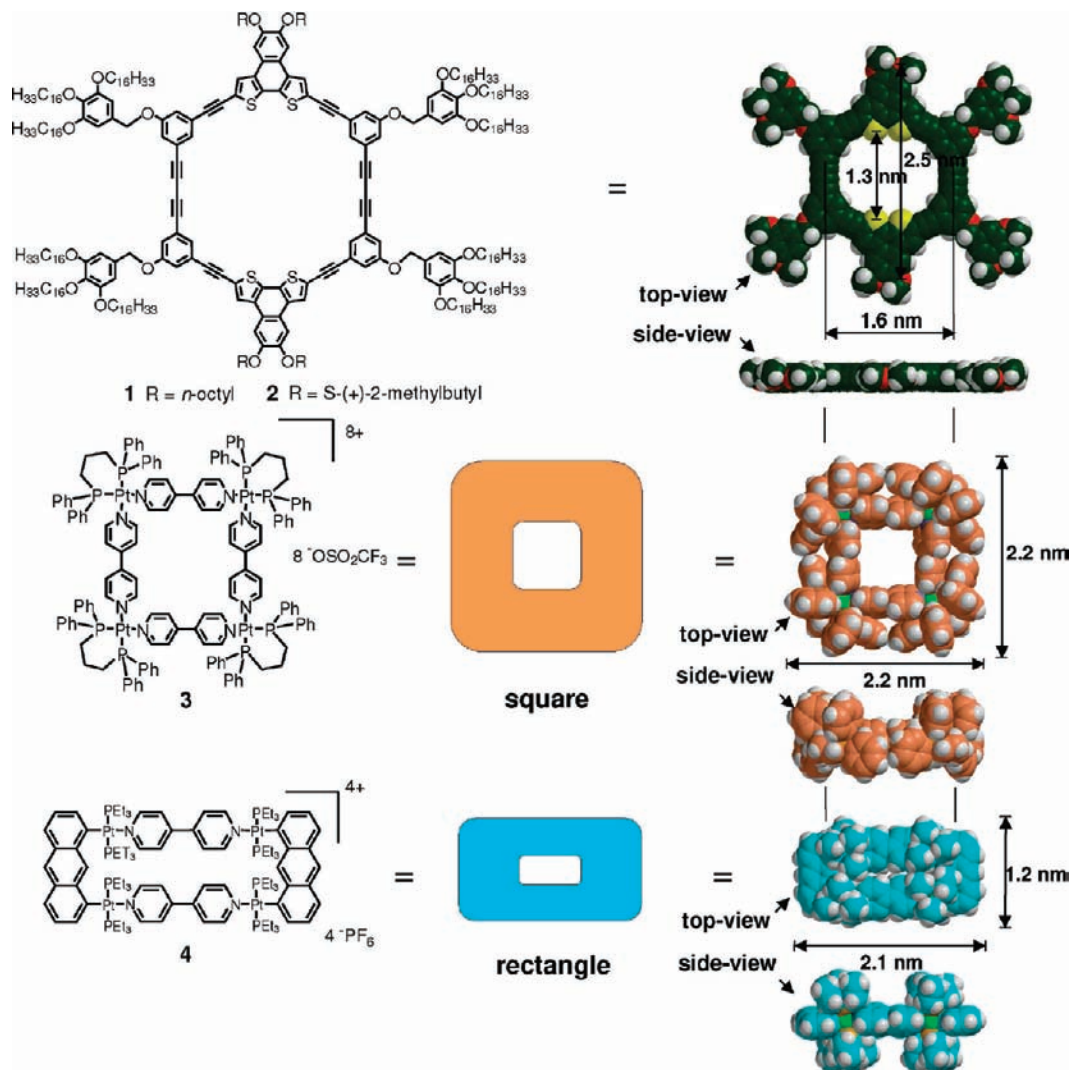
Figure 1. Molecular structures of **1**−**4** and space-filling models with calculated sizes.

macrocycles, whereas the dark stripes are occupied by the alkyl chains. The macrocycles are organized into rows that are separated by the alkyl chains, which are interdigitated and aligned with underlying graphite lattice to maximize the intermolecular interactions (Figure 2b). The overall shape of

the contrast of an individual macrocycle is qualitatively comparable with the electronic density of the frontier orbitals of **1** (see the Supporting Information). The four extraannular groups with oligo-alkyl side chains are also visible and highlighted with green circles. These data strongly indicate that the macrocycles are flat adsorbed at the graphite.[5b] The parameters of an oblique unit cell were determined as $a = 4.5 \pm 0.1$ nm, $b = 5.0 \pm 0.1$ nm, and $\alpha = 72 \pm 1°$ (Figure 2c) and agree well with the calculated molecular size of **1** (Figure 1). Figure 2c shows a tentatively proposed structural model for the ordered monolayer of **1**.

At higher macrocycle concentration, the formation of bilayers can be observed. Figure 3a displays two different types of

(5) (a) Kromer, J.; Rios-Carreras, I.; Fuhrmann, G.; Musch, C.; Wunderlin, M.; Debaerdemacker, T.; Mena-Osteritz, E.; Bäuerle, P. *Angew. Chem.* **2000**, *112*, 3623. (b) Höger, S.; Bonrad, K.; Mourran, A.; Beginn, U.; Möller, M. *J. Am. Chem. Soc.* **2001**, *123*, 5651. (c) Borissov, D.; Ziegler, A.; Höger, S.; Freyland, W. *Langmuir* **2004**, *20*, 2781. (d) Grave, C.; Lentz, D.; Schäfer, A.; Samori, P.; Rabe, J. P.; Franke, P.; Schlüter, A. D. *J. Am. Chem. Soc.* **2003**, *125*, 6907. (e) Fischer, M.; Lieser, G.; Rapp, A.; Schnell, I.; Mamdouh, W.; De Feyter, S.; De Schryver, F. C.; Höger, S. *J. Am. Chem. Soc.* **2004**, *126*, 214. (f) Kalsani, V.; Ammon, H.; Jäckel, F.; Rabe, J. P.; Schmittel, M. *Chem.—Eur. J.* **2004**, *10*, 5841. (g) Ziegler, A.; Mamdouh, W.; Heyen, A. V.; Surin, M.; Uji-i, H.; Abdel-Mottaleb, M. M. S.; De Schryver, F. C.; De Feyter, S.; Lazzaroni, R.; Höger, S. *Chem. Mater.* **2005**, *17*, 5670. (h) Furukawa, S.; Uji-i, H.; Tahara, K.; Ichikawa, T.; Sonoda, M.; De Schryver, F. C.; Tobe, Y.; De Feyter, S. *J. Am. Chem. Soc.* **2006**, *128*, 3502. (i) Jung, S.-H.; Pisula, W.; Rouhanipour, A.; Räder, H. J.; Jacob, J.; Müllen, K. *Angew. Chem.* **2006**, *118*, 4801. (j) Tahara, K.; Johnson II, C. A.; Fujita, T.; Sonoda, M.; De Schryver, F. C.; De Feyter, S.; Haley, M. M.; Tobe, Y. *Langmuir* **2007**, *23*, 10190. (k) Schmittel, M.; Kalsani, V.; Michel, C.; Mal, P.; Ammon, H.; Jäckel, F.; Rabe, J. P. *Chem.—Eur. J.* **2007**, *13*, 6223. (l) Lei, S.; Tahara, K.; De Schryver, F. C.; Van der Auweraer, M.; Tobe, Y.; De Feyter, S. *Angew. Chem.* **2008**, *120*, 3006.

(6) (a) Pan, G.-B.; Cheng, X.-H.; Höger, S.; Freyland, W. *J. Am. Chem. Soc.* **2006**, *128*, 4218. (b) Mena-Osteritz, E.; Bäuerle, P. *Adv. Mater.* **2006**, *18*, 447. (c) Furukawa, S.; Tahara, K.; De Schryver, F. C.; van der Auweraer, M.; Tobe, Y.; De Feyter, S. *Angew. Chem.* **2007**, *119*, 2889. (d) Tahara, K.; Lei, S.; Mössinger, D.; Kozuma, H.; Inukai, K.; Van der Auweraer, M.; De Schryver, F. C.; Höger, S.; Tobe, Y.; De Feyter, S. *Chem. Commun.* **2008**, 3897. (e) Tahara, K.; Lei, S.; Mamdouh, W.; Yamaguchi, Y.; Ichikawa, T.; Uji-i, H.; Sonoda, M.; Kirose, K.; De Schryver, F. C.; De Feyter, S.; Tobe, Y. *J. Am. Chem. Soc.* **2008**, *130*, 6666. (f) Lei, S.; Tahara, K.; Feng, X.; Furukawa, S.; De Schryver, F. C.; Müllen, K.; Tobe, Y.; De Feyter, S. *J. Am. Chem. Soc.* **2008**, *130*, 7119. (g) Schmaltz, B.; Rouhanipour, A.; Räder, H. J.; Pisula, W.; Müllen, K. *Angew. Chem.* **2009**, *121*, 734.
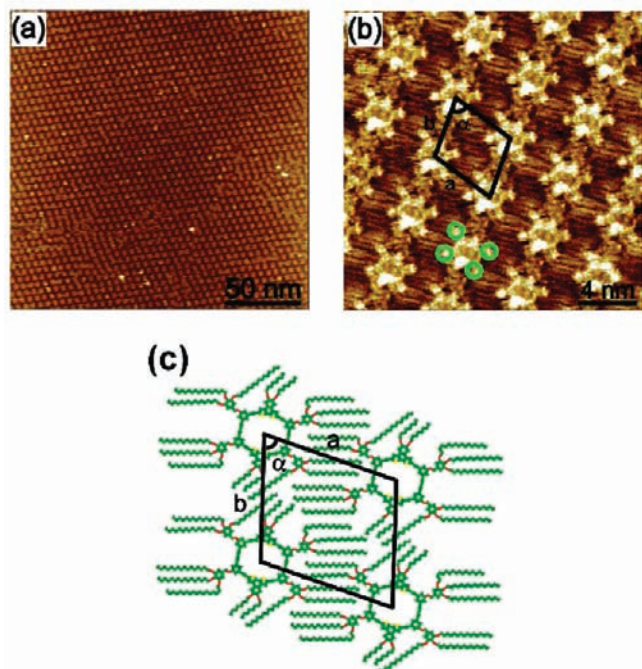
Figure 2. Ordered monolayers of **1** on HOPG at a concentration of ca. 0.5×10^{-5} M. (a) Large-scale STM image. $V_{bias} = 764$ mV; $I_t = 506$ pA. (b) Higher-resolution STM image. $V_{bias} = 408$ mV; $I_t = 694$ pA. The four extraannular groups are indicated with green circles. (c) Proposed structural model. An oblique unit cell is indicated in black.

Figure 3. Ordered bilayers of **1/1** on HOPG at a concentration of ca. 5×10^{-5} M. (a) Typical STM image. $V_{bias} = 1.23$ V; $I_t = 201$ pA. (b) A composite STM image, in which the tunneling parameters have been changed at the dashed white line, showing the underlying and upper layers simultaneously. The scanning direction was from top to bottom. Upper region: $V_{bias} = 1.2$ V; $I_t = 201$ pA. Lower region: $V_{bias} = 600$ mV; $I_t = 201$ pA. (c) A section analysis along the white line in a is displayed in c.

appearance of the macrocycles with the cross-section analysis. This might be either due to the different adsorption registry or the formation of a bilayer **1/1**.[11] Once a monolayer is formed, it can act as a template for the epitaxial adsorption of an additional layer of macrocycles. Figure 3b shows a composite STM image, in which the underlying and upper layers are shown simultaneously. Apparently, the macrocycle molecules are located on top of the first monolayer. The alkyl chains for the second layer are not resolved. Nevertheless, they should be located between the adjacent molecular rows and are interdigitated according to the lattice parameter. Similar phenomena have also been observed in the self-assembly of alkyl-substituted tetrathiafulvalene.[12] It has to be noted that only small ordered domains could be found for the bilayer structures in the present experiments. Within experimental errors, the parameters of an oblique unit cell of **1/1** are identical to those of **1**, indicating
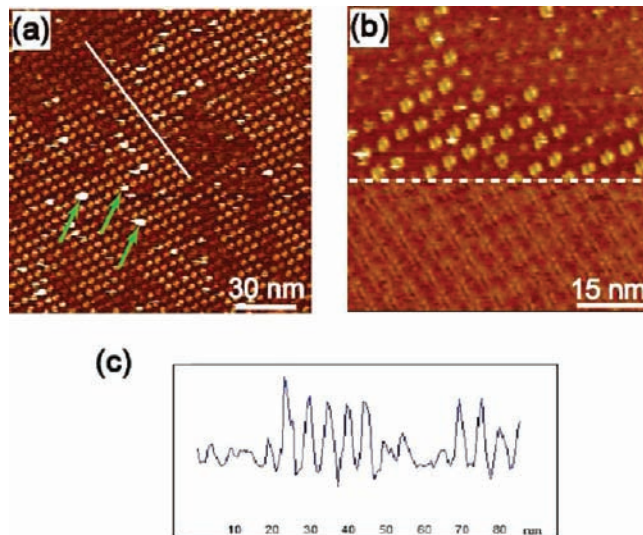
that the first monolayer of **1** is stable enough to act as a template. In addition, some macrocycle cores, indicated with the green arrows, appear brighter at random places in the image, though always close to the molecular row. The number of such brighter spots increases a little with increasing macrocycle concentration. This effect can be attributed to the adsorption of more than two macrocycle cores on top of each other.

Because **1** and **2** contain (electron-rich) polycyclic bithiophene units in their backbone, the macrocycle pattern at the HOPG surface is an ideal platform to act as template for the deposition of (electron deficient) guest molecules. After recording the ordered monolayer of **1** (Figure 2a) at the 1-phenyloctane/HOPG interface, a drop ($\sim$0.5 μL) of a solution of the square metallacycle **3** in 1-phenyloctane was directly added. Figure 4a shows a typical large-scale STM image recorded about 10 min after adding the solution. The well-ordered bright spots are an interesting feature of the array, a significant difference from the array of **1** discussed before. They result either from a bi- or multilayer structure of **1** or from an epitaxialy grown commensurable adlayer of **3** on a monolayer of **1** (**1/3**).[13,14] The latter is most likely, because first only the ordered monolayers of **1** have been observed before adding the solution of metallacycle **3**. Second, only the monolayer structures of **1** could be recorded when other guests such as C_{60}, triphenylene, perylene, coronene, or TCNQ were added by using the same experimental procedure as for **3**. And finally, only small-ordered domains with sporadically distributed brighter spots could be observed

(7) (a) Li, S.-S.; Yan, H.-J.; Wan, L.-J.; Yang, H.-B.; Northrop, B. H.; Stang, P. J. *J. Am. Chem. Soc.* **2007**, *129*, 9268. (b) Li, S.-S.; Northrop, B. H.; Yuan, Q.-H.; Wan, L.-J.; Stang, P. J. *Acc. Chem. Res.* **2009**, *42*, 249. (c) Gong, J.-R.; Wan, L.-J.; Yuan, Q.-H.; Jude, H.; Stang, P. J. *Proc. Natl. Acad. Sci. U.S.A.* **2005**, *102*, 971. (d) Yuan, Q.-H.; Wan, L.-J.; Jude, H.; Stang, P. J. *J. Am. Chem. Soc.* **2005**, *127*, 16279.

(8) (a) Stang, P. J.; Cao, D. H.; Saito, S.; Arif, A. M. *J. Am. Chem. Soc.* **1995**, *117*, 6273. (b) Stang, P. J.; Olenyuk, B. *Acc. Chem. Res.* **1997**, *30*, 501. (c) Kuehl, C. J.; Huang, D.; Stang, P. J. *J. Am. Chem. Soc.* **2001**, *123*, 9634.

(9) (a) Tovar, J. D.; Swager, T. M. *Adv. Mater.* **2001**, *13*, 1775. (b) Tovar, J. D.; Rose, A.; Swager, T. M. *J. Am. Chem. Soc.* **2002**, *124*, 7762.

(10) (a) Glaser, C. *Ber. Dtsch. Chem. Ges.* **1869**, *2*, 422. (b) Sondheimer, F.; Wolovsky, R. *J. Am. Chem. Soc.* **1962**, *84*, 260. (c) Sondheimer, F. *Acc. Chem. Res.* **1972**, *3*, 81. (d) O'Krongly, D.; Denmeade, S. R.; Chiang, M. Y.; Breslow, R. *J. Am. Chem. Soc.* **1985**, *107*, 5544. (e) Kadei, K.; Vögtle, F. *Chem. Ber.* **1991**, *124*, 909. (f) Höger, S.; Enkelmann, V. *Angew. Chem.* **1995**, *107*, 2917. (g) Siemsen, P.; Livingston, R. C.; Diederich, F. *Angew. Chem.* **2000**, *112*, 2740.

(11) The term **1/1** describes a monolayer of **1** on a substrate (here HOPG) that acts as template for the adsorption of a second monolayer, in this specific case again of **1**, so that a double layer is formed.

(12) (a) Lu, J.; Zeng, Q.-D.; Wang, C.; Wan, L.-J.; Bai, C.-L. *Chem. Lett.* **2003**, *32*, 856. (b) Abdel-Mottaleb, M. M. S.; Gomar-Nadal, E.; Surin, M.; Uji-i, H.; Mamdouh, W.; Veciana, J.; Lemaur, V.; Rovira, C.; Cornil, J.; Lazzaroni, R.; Amabilino, D. B.; De Feyter, S.; De Schryver, F. C. *J. Mater. Chem.* **2005**, *15*, 4601.

(13) Accordingly, the term **1/3** describes a monolayer of **1** on a substrate (here HOPG) that acts as template for the adsorption of a second monolayer, in this specific case of **3**.

(14) (a) Stöhr, M.; Wagner, T.; Gabriel, M.; Weyers, B.; Möller, R. *Adv. Funct. Mater.* **2001**, *11*, 175. (b) Hooks, D. E.; Fritz, T.; Ward, M. D. *Adv. Mater.* **2001**, *13*, 227.
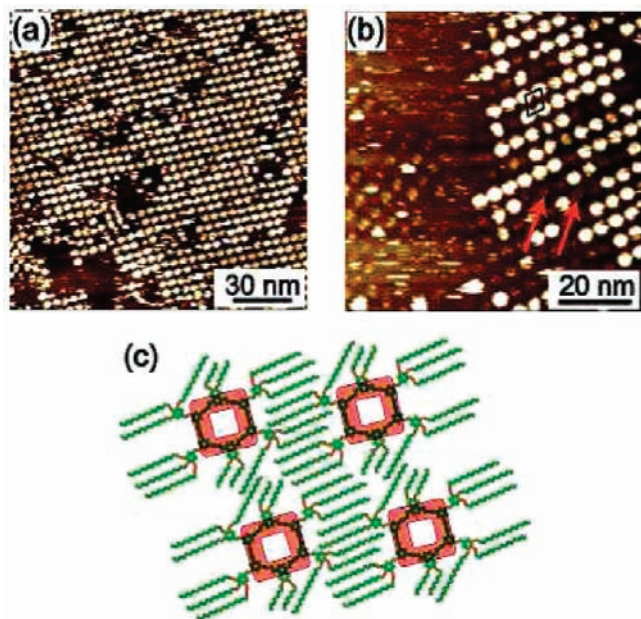
Figure 4. Ordered arrays of **1/3** on HOPG. (a) Large scale STM image. $V_{bias} = 1.30$ V; $I_t = 195$ pA. (b) High resolution STM image. $V_{bias} = 1.38$ V; $I_t = 189$ pA. (c) Proposed structural model. Each red square stands for one metallacycle.
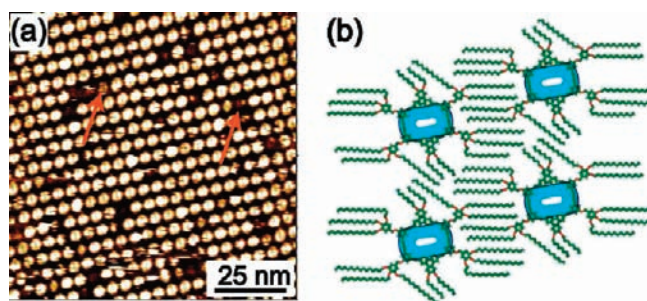

Figure 5. Ordered arrays of **1/4** on HOPG. (a) Typical STM image of **1/4**. $V_{bias} = 1.17$ V; $I_t = 201$ pA. The red arrows indicate the underlying macrocycle molecules **1**. (b) Proposed structural model. The blue rectangles indicate the position of **4** at the template **1**.

for the second layers of **1** although different (even high) concentrations of **1** have been investigated. This is not the case for the ordered structure of **1** laced with a solution of **3** that can form large-ordered domains. Therefore, we strongly assume that the above observations demonstrate the formation of a bicomponent architecture of **1/3**.

Figure 4b is a higher-resolution STM image and reveals details of the internal molecular structure and orientation of the composite structure. The underlying macrocycles are indicated with red arrows. It is clear that the metallacycles are not included in the intrinsic molecular void of **1**, but located above the macrocycles to form the second layer. Additionally, for each macrocycle, only one square metallacycle can be detected. This is reasonable because the intraannular cavity of **1** is not large enough to accommodate a metallacycle (Figure 1).

Similar assembling behavior has been observed for the metallacycle **4** on the ordered monolayer of **1**. Figure 5a shows a typical STM image of an ordered bilayer of **1/4**. Each bright spot in the image is associated with an individual molecule of **4** on an underlying layer of **1** and the bright spot is located above the center of macrocycle **1**. Figures 4c and 5b show schematic models for the ordered bilayers of **1/3** and **1/4**,
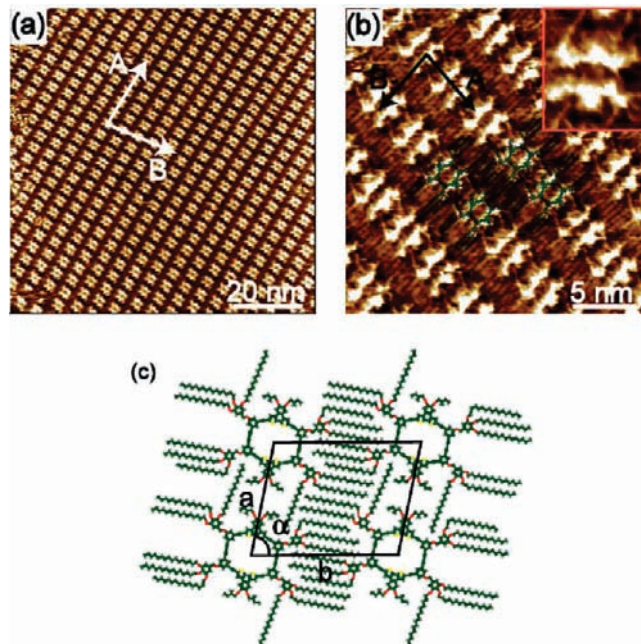
Figure 6. Ordered monolayers of **2** on HOPG. (a) Large-scale STM image. $V_{bias} = 578$ mV; $I_t = 683$ pA. (b) Higher resolution STM image. $V_{bias} = 529$ mV; $I_t = 717$ pA. The inset is a close-up image of one macrocycle molecule. (c) Proposed structural model. An oblique unit cell is indicated in black.

respectively. Within experimental errors, the data of an oblique unit cell, containing either one square **3** or one rectangle **4**, are identical to those of pure **1**. These observations indicate that the structural information of the macrocycle layer is perfectly transformed to the guest molecules and that the first monolayer of **1** is stable enough to act as a template for the adsorption of metallacycles **3** and **4**. It should be noted that unlike a previous study on the macrocycle/fullerene system (1: 2 stoichiometrty),[6a] the formation of bicomponent architectures of **1/3** and **1/4** has led to a 1:1 stoichiometrty.

To explore the generality of the formation of the macrocycle/metallacycles bicomponent structures, the aforementioned experimental procedures have also been applied for the deposition of **2**, **2/3**, and **2/4**. Figure 6a represents a large-scale STM image of the ordered monolayer of **2**.

Similar to the macrocycle **1**, the bright protrusions in the STM image are attributed to the unsaturated backbone of the macrocycles, whereas the dark stripes are occupied by the alkyl chains. The macrocycles are organized into rows that are separated by the alkyl chains which are interdigitated and aligned with the underlying graphite lattice to maximize the intermolecular interaction (Figure 6b). The macrocycles are flat adsorbed at the graphite in order to maximize the molecule−substrate interaction. Figure 6c is a tentatively proposed structural model for the ordered monolayer of **2**. The parameters of an oblique unit cell were determined as $a = 3.9 \pm 0.1$ nm, $b = 5.0 \pm 0.1$ nm, and $\alpha = 78 \pm 2°$. These data are slightly different from those of **1**. This can be attributed to the different groups, n-octyl versus 2-methylbutyl, at the polycyclic bithiophene units of the two macrocycles (Figure 1). Moreover, the existence of the methylbutyl groups can hinder the formation of a bilayer **2/2**. In the present study, only sporadically distributed brighter spots have been observed for the bilayer **2/2**, even at higher macrocycle concentrations. This is possibly because the presence of
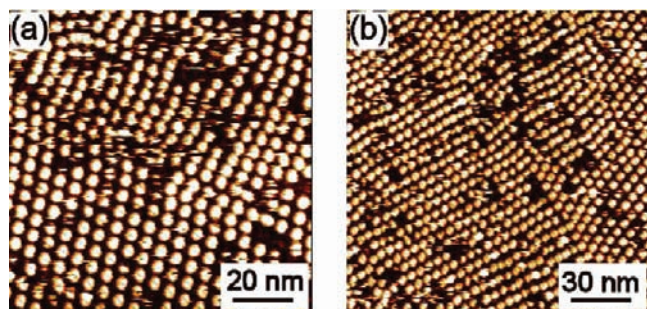
Figure 7. Typical STM images of (a) **2/3** and (b) **2/4** on HOPG. (a) V_{bias} = 1.30 V; I_t = 195 pA. (b) V_{bias} = 1.38 V; I_t = 189 pA. The unit-cell parameters of both **2/3** and **2/4** ($a = 3.9 \pm 0.1$ nm, $b = 5.0 \pm 0.1$ nm, and $\alpha = 78 \pm 2°$) are the same as those for **2** within experimental errors.

the branched 2-methylbutyl groups reduces the $\pi-\pi$ interaction between the macrocycle cores compared to the linear n-octyl groups.

After recording the ordered monolayer of **2** at the 1-phenyl-octane/HOPG interface, a drop (~0.5 µL) of a solution of either square metallacycle **3** or rectangular metallacycle **4** in 1-phenyloctane was directly added. Figure 7 show typical STM images of **2/3** and **2/4** recorded about 10 min after adding the solution. Again, the well-ordered bright spots are an interesting feature of the array, a significant difference from the array of pure **2**. As discussed above, the macrocycles **2** themselves could not form large ordered domains of a bilayer structure. These bilayer structures are thus from a bicomponent architecture of **2/3** and **2/4**, respectively. As for the composite structures of **1**, for each macrocycle **2**, only one metallacycle, either square **3** or rectangle **4**, can be detected. In all cases, the bithiophene macrocycles determine the distance between adjacent coadsorbed metallacycles, indicating that the bithiophene macrocycles play an important role in determining the lattice constants of the ordered bicomponent architectures of **2/3** and **2/4**.

Although the metallacycles **3** and **4** are nonplanar, their deposition and codeposition on solid surfaces has been reported recently.[7b] As far as pure metallacycles **3** and **4** on HOPG are concerned, only disordered layers have been observed (see the Supporting Information). Therefore, and because of the sizes of the macrocycles and the metallacycles, the driving force for

the formation of this superstructure is not the interaction of the metallacycles with the uncovered HOPG surface inside the rings. At present, the driving force for the formation of ordered structures of **1/3**, **1/4**, and **2/3**, **2/4**, respectively, is not understood yet and will be the object of further investigations. One might speculate that the electron-rich units of the bithiophene macrocycle can electronically favorably interact with electron-deficient parts of the metallacycles as well as the diffusion barrier formed by the primary layers of macrocycle **1** and **2**.

Conclusions

2D ordered arrays of shape-persistent macrocycle and macrocycle/metallacycles (1:1) have been obtained on HOPG by self-assembly under ambient conditions. The ordered macrocycle array acts as a template for the epitaxial deposition of the adlayer molecules. For each underlying macrocycle, one metallacycle molecule has been detected and the structural information of the macrocycle layer is perfectly transformed to the guest molecules. The driving force can be that the electron rich units of the bithiophene macrocycle electronically favorably interact with the electron deficient parts of the metallacycles as well as the diffusion barrier formed by the primary layer of macrocycles. A rather unexpected observation is that the present compound could not be coadsorbed with C_{60}, indicating that only a minor change in the structure of the macrocycle has a dramatic effect on the ability of the monolayer to bind additional guest molecules. At present, the as-prepared 2D-supramolecular structures are used as a template for complex 3D structures.

Supporting Information Available: Additional STM, synthesis, characterization, and molecular modeling of **1** and **2**. This material is available free of charge via the Internet at http://pubs.acs.org.

JA907220F